females stain blue with a distinct red nucleus [P. C. C. Garnham, *Malaria Parasites and Other Haemosporidia* (Blackwell Scientific, Oxford, 1966)]. Sex ratios based on counts of 50 to 75 gametocytes were found to be representative. We calculated sex ratios from either 50,000 RBCs or 100 gametocytes, whichever was less. Sex ratios are given as proportion of males.

7. R. E. Sinden, G. A. Butcher, O. Billker, S. L. Fleck,. *Adv. Parasitol.* **38**, 53 (1996).
8. R. Carter, R. W. Gwadz, F. M. McAuliffe, *Exp. Parasitol.* **47**, 185 (1979).
9. Infection classification by day with respect to peak parasitemia is retrospective, where $P - 1$, $P - 2$, and $P - 3$ are 1, 2, and 3 days before peak parasitemia. Erythropoietic treatments were carried out on the first day parasites appeared in the blood (parasite patency) and infection peak was not always the same number of days after parasite patency. Hence, treatment with respect to day of peak parasitemia varied, and that information is supplied in the figure legends. Such variation was taken into account in the statistical analyses.
10. Polynomial regression was performed in SIMSTAT for Windows (Provalis Research).
11. K. P. Day, R. E. Hayward, M. Dyer, *Parasitology* **116**, S95 (1998).
12. Two vaccination procedures were carried out according to protocols previously established (*8*) [R. Carter, R. W. Gwadz, I. Green, *Exp. Parasitol.* **47**, 194 (1979); D. C. Kaushal *et al.*, *J. Immunol.* **131**, 2557 (1983)]. Chickens received intravenous injections with x-irradiated (35 Krad) purified male gametes or a mixture of female gametes and microgametocytes, which are not separable. Each vaccination type was administered three times over 3 weeks per chicken host (n = 3 for both treatments) before intravenous injection of live parasitized blood.
13. Statistical analyses were conducted with the statistical package Genstat 5.4.1. Because each individual vertebrate host was included in the data set many times, we corrected for repeated measures by fitting a generalized linear mixed model (GLMM procedure) with a Poisson error structure with "animal" as the only term in the random model. For both the sex ratio and oocyst analyses, the data were overdispersed and so were corrected for by estimating a dispersion parameter for each analysis [M. J. Crawley, *GLIM for Ecologists* (Blackwell Scientific, Oxford, 1993)]. All analyses of the effects of sex ratio on infectivity were controlled for gametocyte density, infection outcome (live or die), day of infection with respect to day of peak parasitemia, and individual host. Statistical significance was presented as Walds statistics, which are equivalent to a χ^2 analysis. Between-treatment comparisons were performed with respect to peak parasitemia up to, but not including, the day of peak parasitemia, at which time any erythropoietic treatment effects were disguised by the erythropoietic response normally associated with infection control. For clarity, Figs. 1 and 4 show treatment means.
14. Five- to seven-day-old *Aedes aegypti* (Liverpool Blackeye strain) were used for the mosquito infection studies. Oocyst counts in mosquitoes were made 7 days postinfection on midguts dissected from 30 gravid females and then stained with 0.5% mercurochrome.
15. Mosquito infectivity: between-treatment comparisons were done by day with respect to peak parasitemia specifying a Poisson error structure (which gives the same fit as a negative binomial) [K. Wilson, B. T. Grenfell, D. J. Shaw, *Funct. Ecol.* **10**, 592 (1996)] for the distribution of oocyst counts per mosquito per chicken. For clarity, Fig. 3 shows treatment geometric means with 99% confidence intervals.
16. F. Hawking, K. Gammage, M. J. Worms, *Trans. R. Soc. Trop. Med. Hyg.* **65**, 189 (1972).
17. Reticulocyte-rich blood was injected intravenously in exchange for blood (20% of total blood volume) taken from an infected chicken host, thereby increasing the proportion of RBCs that were reticulocytes without stimulating erythropoiesis (n = 6). Reticulocytes were obtained from chickens 72 hours after subcutaneous injection of the hemolytic drug phenylhydrazine hydrochloride (Sigma) at a dose of 6 mg per 100 g of body weight; the blood was washed in 1× phosphate-buffered saline (0.14 M NaCl, 2.7 mM KCl, 1.5 mM KH_2PO_4, 8,1 mM Na_2HPO_4), and the volume was restored with serum from naive chickens.
18. S. L. Schindler and R. P. Gildersleeve, *Comp. Biochem. Physiol. A Comp. Physiol.* **87**, 533 (1987).
19. Two methods were used to induce erythropoiesis: exsanguination of 20% to 30% of total blood volume by cardiac puncture on the day of parasite patency (>0.1% parasitemia) (n = 6), and 16 hours of exposure to mildly hypoxic conditions on the day of patency (15% oxygen, 85% nitrogen; Carboxyque, France) (n = 8); W. F. Rosse and T. A. Waldmann, *Blood* **27**, 654 (1966).
20. J. S. Milledge and P. M. Cotes, *J. Appl. Physiol.* **59**, 360 (1985); H. Pagel, A. Engel, W. Jelkmann, *Adv. Exp. Med. Biol.* **317**, 515 (1992); M. J. McGuire and J. L. Spivak, in *The Fundamentals of Clinical Hematology*, J. L. Spivak and E. R. Eichner, Eds. (Johns Hopkins Univ. Press, London, 1993), pp. 117–128.
21. R. E. L. Paul, A. Raibaud, P. T. Brey, *Parassitologia* **41**, 153 (1999).
22. W. Jelkmann, *Clin. Invest.* **72**, S3 (1994).
23. Two methods were used to induce erythropoiesis in mice: intraperitoneal injection of mouse recombinant Epo (Boehringer Mannheim, France) at a concentration of 70 or 700 units/liter administered in 100 μl of 0.9% NaCl on the 3 days after parasite patency, and 16 hours of exposure to mildly hypoxic conditions on the day of patency (15% oxygen, 85% nitrogen) (n = 5 for each treatment and n = 10 for control infections).
24. E. Geiringer, *Proc. Soc. Exp. Biol. Med.* **106**, 752 (1961).
25. A. M. el Hassan, A. M. Saeed, J. Fandrey, W. Jelkmann, *Eur. J. Haematol.* **59**, 299 (1997).
26. Supported by Institut Pasteur, Paris. R.E.L.P. was supported by the Medical Research Council (UK)/CNRS, Fondation pour la Recherche Médicale, and a European Commission Training and Mobility of Researchers Marie Curie Research Training Grant. We thank A. Danchin, G. Milon, P. Langlade-Demoyen, C. Roth, P. Druilhe, C. Lazure, K. Kean, and S. Cole for helpful discussions and A. Carmi-Leroy for mosquito rearing.

14 September 1999; accepted 17 November 1999

DNA Topoisomerase IIβ and Neural Development

Xia Yang,[1]* Wei Li,[2]*† Elizabeth D. Prescott,[1]‡ Steven J. Burden,[1] James C. Wang[2]

DNA topoisomerase IIβ is shown to have an unsuspected and critical role in neural development. Neurogenesis was normal in IIβ mutant mice, but motor axons failed to contact skeletal muscles, and sensory axons failed to enter the spinal cord. Despite an absence of innervation, clusters of acetylcholine receptors were concentrated in the central region of skeletal muscles, thereby revealing patterning mechanisms that are autonomous to skeletal muscle. The defects in motor axon growth in IIβ mutant mice resulted in a breathing impairment and death of the pups shortly after birth.

Murine DNA topoisomerase IIβ (IIβ) is a member of the type II DNA topoisomerase subfamily that mediates the passage of one DNA double helix through another (*1*). Yeasts and *Drosophila* possess a single type II DNA topoisomerase, which is indispensable for segregation of intertwined pairs of newly replicated chromosomes (*2*). In yeasts, the enzyme also shares the function of DNA topoisomerase I in relieving torsional and flexural strains in DNA. Simultaneous inactivation of DNA topoisomerases I and II severely affects DNA and ribosomal RNA synthesis and arrests cell growth irrespective of the stage of cell cycle (*3*).

In mammals there are two closely related type II topoisomerases, IIα and IIβ, encoded by distinct genes (*1*). The IIα rather than the IIβ isoform appears to unlink DNA during chromosome segregation. Cell lines expressing IIα but not IIβ have been identified, indicating that IIβ is dispensable in cellular processes (*4*). To determine the role of IIβ in vivo, we disrupted the murine *TOP2*β gene according to standard procedures (*5*). Two adjacent exons in one copy of *TOP2*β in embryonic stem cells, one of which contains the active-site tyrosine codon, were replaced by the neomycin-resistance marker (Fig. 1A) [see supplementary Web material (*6*) for details on targeting vector construction]. Germ line chimeras from blastocysts injected with the mutated cells were then used to obtain heterozygous *top2*$\beta^{+/-}$ mice (*5*). Whereas *top2*$\beta^{+/-}$ mice are phenotypically indistinquishable from their wild-type (WT) littermates, homozygous *top2*$\beta^{-/-}$ embryos from intercrosses of the heterozygotes are dead at birth. Genotypying of a total of 194 progeny from these intercrosses identified 46 *top2*$\beta^{-/-}$ homozygotes among 50 perinatally dead pups, and none among the 144 surviving neonates. Analysis of mRNA from the liver of an embryonic day 18.5 (E18.5) *top2*$\beta^{-/-}$ embryo showed no detectable IIβ transcript [Web figure 1 (*6*)], and antibodies specific to

[1]Skirball Institute of Molecular Medicine, New York University Medical School, 540 First Avenue, New York, NY 10016, USA. [2]Department of Molecular and Cellular Biology, Harvard University, 7 Divinity Avenue, Cambridge, MA 02138, USA.

*These authors contributed equally to this work.
†Present address: Vertex Pharmaceuticals, 40 Allison Street, Cambridge, MA 02139, USA.
‡Present address: Department of Biochemistry and Biophysics, University of California at San Francisco, 513 Parnassus Avenue, San Francisco, CA 94143, USA.

IIβ detected the protein in extracts of fibroblasts from E13.5 WT but not *top2*β$^{-/-}$ embryos (*7*). Wild-type and *top2*β$^{-/-}$ embryos are comparable in size up to E15.5, but homozygous mutant embryos show retarded growth thereafter; at E18.5 the average weight of *top2*β$^{-/-}$ embryos is ~65% that of their WT littermates. The *top2*β$^{-/-}$ embryos also exhibit a curled appearence because of an abnormal curvature of their vertebral columns (Fig. 1B). Examination of the *top2*β$^{-/-}$ embryos showed no gross morphological abnormality in major organs. These embryos, however, lacked spontaneous and tactile-stimulated movements. Their lung aveoli remained collapsed after birth, indicating that a respiratory failure is the most likely cause of their perinatal death.

The failure of *top2*β$^{-/-}$ newborns to move or breathe suggested a defect in neuromuscular function. The number of motor neurons or interneurons in WT and mutant embryos at E12.5 appears to be similar, as revealed by staining spinal sections with appropriate antibodies. Furthermore, in E12.5 *top2*β$^{-/-}$ embryos, sensory as well as motor neurons extend their axons into the periphery; motor axons, specifically labeled by injecting DiI (1,1′-dioctadecyl-3,3,3′,3′-tetramethylindocarbocyanine perchlorate) into the ventral spinal cord (*8*), project into the limbs by E12.5 and continue to grow further into the limbs by E13.5 [Web figure 2 (*6*)]. Thus, early aspects of motor neuron differentiation, including neurogenesis, appear normal in *top2*β$^{-/-}$ embryos.

We studied neuromuscular synapses in *top2*β$^{-/-}$ embryos by staining whole mounts of diaphragm muscles with probes that allowed us to assess presynaptic and postsynaptic differentiation (*9*): a mixture of antibodies to neurofilaments (NF) and a synaptic vesicle protein synaptophysin (Syn) was used to stain axons and nerve terminals, respectively, and α-bungarotoxin (α-BGT) was used to stain postsynaptic acetylcholine receptors (AChRs). In WT mice, motor axons branch and terminate adjacent to the main intramuscular nerve, resulting in a narrow, well-defined endplate zone in the middle of the diaphragm muscle (Fig. 2A). Presynaptic nerve terminals precisely overlie the postsynaptic membrane, which contains a high concentration or cluster of AChRs (Fig. 2A).

In E18.5 *top2*β$^{-/-}$ embryos, presynaptic nerve terminals and axons are absent from the diaphragm muscle (Fig. 2A). Similar results were obtained by staining longitudinal sections of limb muscles from mutant embryos (*7*). We considered the possibility that early motor axons failed to reach their skeletal muscle targets or that these axons contacted muscle and subsequently withdrew. Staining of whole mounts of diaphragm muscles at E13.5, E15.5, and E18.5 revealed that motor axons in the mutant embryos extended toward the diaphragm muscle but failed to grow or branch within the muscle at all stages examined (Fig. 2B). In contrast, motor axons in WT embryos reached the diaphragm muscle by E13.5 and continued to grow within the muscle and to form a well-patterned endplate zone (Fig. 2B). These data indicate that motor axons in *top2*β$^{-/-}$ embryos reach their skeletal muscle targets but fail to grow or branch within their limb and diaphragm muscles and to contact differentiating muscle fibers.

The presence of primary nerve trunks but not secondary branches in the developing limbs of *top2*β$^{-/-}$ embryos is reminiscent of the motor axon pattern in muscle-less limbs (*10*), and points to a plausible defect in communication between muscle cells and motor axons in the mutant embryos. Because growth of nociceptive sensory neurons that innervate skin and not muscle is also defective in *top2*β$^{-/-}$ embryos (see below), we favor the idea that IIβ is required in neurons, rather than in muscles, for the expression of molecules essential for receiving cues for axon growth and branching within the target tissue.

Surprisingly, despite an absence of synapses in the diaphragm muscle of *top2*β$^{-/-}$ embryos, AChR clusters are enriched in a band near the middle of the muscle (Fig. 2A), rather than distributed uniformly along the length of muscle fibers. Current ideas of synapse formation suggest that nerve-derived signals are required to induce synaptic differentiation (*11*). Our results, however, suggest that the expression pattern of AChR clusters in skeletal muscles is determined, at least in part, by mechanisms that are autonomous to muscle. Consistent with this idea, although *top2*β$^{-/-}$ embryos lack axons and nerve terminals in both right and left hemi-diaphragms (Fig. 2A), AChR clusters are distributed more widely in the right than in the left hemi-diaphragm (Fig. 2A), like the patterns seen in WT embryos (Fig. 2A). Although it is possible that motor axons, which fail to grow within developing muscle, provide diffusible signals that induce AChR clustering, our results indicate that such signals would act on a muscle that is prepatterned. In principle, this prepattern could arise from separate lineages for synaptic and extrasynaptic myofiber nuclei or from the pattern of muscle growth, in which myoblast fusion at the ends of developing myofibers results in a mature central region and less differentiated distal ends of the muscle (*12*). Further, these results raise the possibility that spatial cues to restrict growing axons to the central region of the muscle could be provided by molecules that are prepatterned in developing muscle.

Although neuromuscular synapses are absent from diaphragm and limb muscles, synaptic sites are readily detected in intercostal muscles of *top2*β$^{-/-}$ embryos (Fig. 2C). Thus, our results indicate that the rules for synapse formation differ between intercostal muscles and limb and diaphragm muscles. Intercostal, limb, and diaphragm muscles are all hypaxial muscles, derived from cells in the lateral

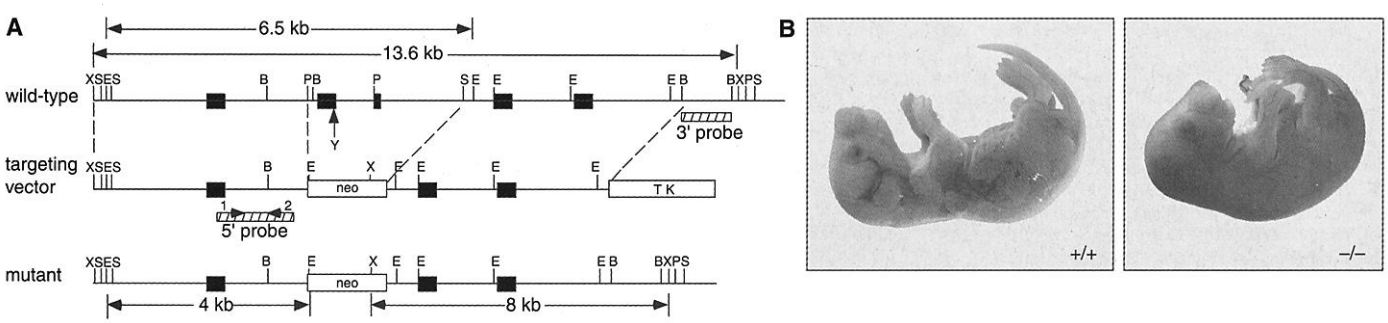

Fig. 1. (**A**) The relevant regions in the WT murine *TOP2*β gene (upper), the neo/TK targeting vector (middle), and the mutated *top2*β allele (lower). Coding stretches are represented by filled boxes; B, E, P, S, and X denote restriction sites of Bam HI, Eco RI, Pst I, Sac I, and Xba I, respectively, and neo and TK denote the neomycin-resistance and thymidine kinase markers. The letter Y (upper) marks the position of the active-site tyrosine codon. The hatched bars mark the positions of probes used in genotyping; the "5′ probe" was prepared by polymerase chain reaction with primers represented by the arrows 1 and 2 [see supplementary Web material (*6*) for details on the construction of the targeting vector and examples of genotyping and mRNA blot-hybridization results]. (**B**) Images of E17.5 WT (left) and *top2*β$^{-/-}$ (right) embryos.

dermomyotome (*13*), but only the precursors for diaphragm and limb muscles express the homeobox gene *Lbx1* and migrate from the somite to the septum transversum or limb, respectively (*14*). Thus, the lack of *top2*β$^{-/-}$ may have different manifestations in muscles of different lineages.

Sensory axon growth, however, is aberrant in intercostal muscles. In WT embryos motor axons branch and terminate adjacent to the main intramuscular nerve, and sensory axons branch toward the rostral rib and terminate near muscle insertions on both sides of the rib (Fig. 3, A to C). NF-stained axons in *top2*β$^{-/-}$ embryos stray from the main nerve and grow profusely across the rib (Fig. 3A). By injecting DiI into the ventral horn of the spinal cord to selectively label motor axons (Fig. 3B), or into dorsal root ganglia to selectively label sensory axons (Fig. 3C), these ectopic axons in *top2*β$^{-/-}$ embryos are shown to be derived from sensory and not motor neurons.

Sensory neuron defects in *top2*β$^{-/-}$ embryos are not restricted to axon growth in skeletal muscle. Proprioceptive sensory neurons extend their primary axons into the ventral region of the spinal cord, where they terminate on interneurons or directly on motor neurons. In addition, these proprioceptive sensory neurons extend collaterals in the dorsal spinal cord, and these collateral axons form the dorsal column that terminates in the medulla. *Top2*β$^{-/-}$ embryos lack the dorsal column (Fig. 3D). Furthermore, axons of nociceptive sensory neurons that project to the dorsal horn of the spinal cord are absent in *top2*β$^{-/-}$ embryos (Fig. 3D). Because nociceptive sensory neurons have their peripheral endings in epidermis and not in skeletal muscle, the failure of these neurons to project within the spinal cord is unlikely to be owing to a requirement of the enzyme in skeletal muscles. Because these axons are absent from the spinal cord as early as E14.5 (*7*), the time of their normal projection into the spinal cord, sensory axons in *top2*β$^{-/-}$ embryos apparently fail to initiate growth within the spinal cord, rather than entering and withdrawing at later stages.

The pronounced neural and neuromuscular abnormalities in the *top2*β$^{-/-}$ embryos are observed at late stages of embryogenesis when neuron and muscle cells are well differentiated. Thus, these defects are unlikely to reflect a general replicative or transcriptional role of IIβ. Defects in neurogenesis, associated with an increase in apoptosis, are also evident in mice lacking XRCC4 or DNA ligase IV (*15, 16*). XRCC4 protein and DNA ligase IV are components in a DNA repair complex, and thus their effects on neurogenesis may re-

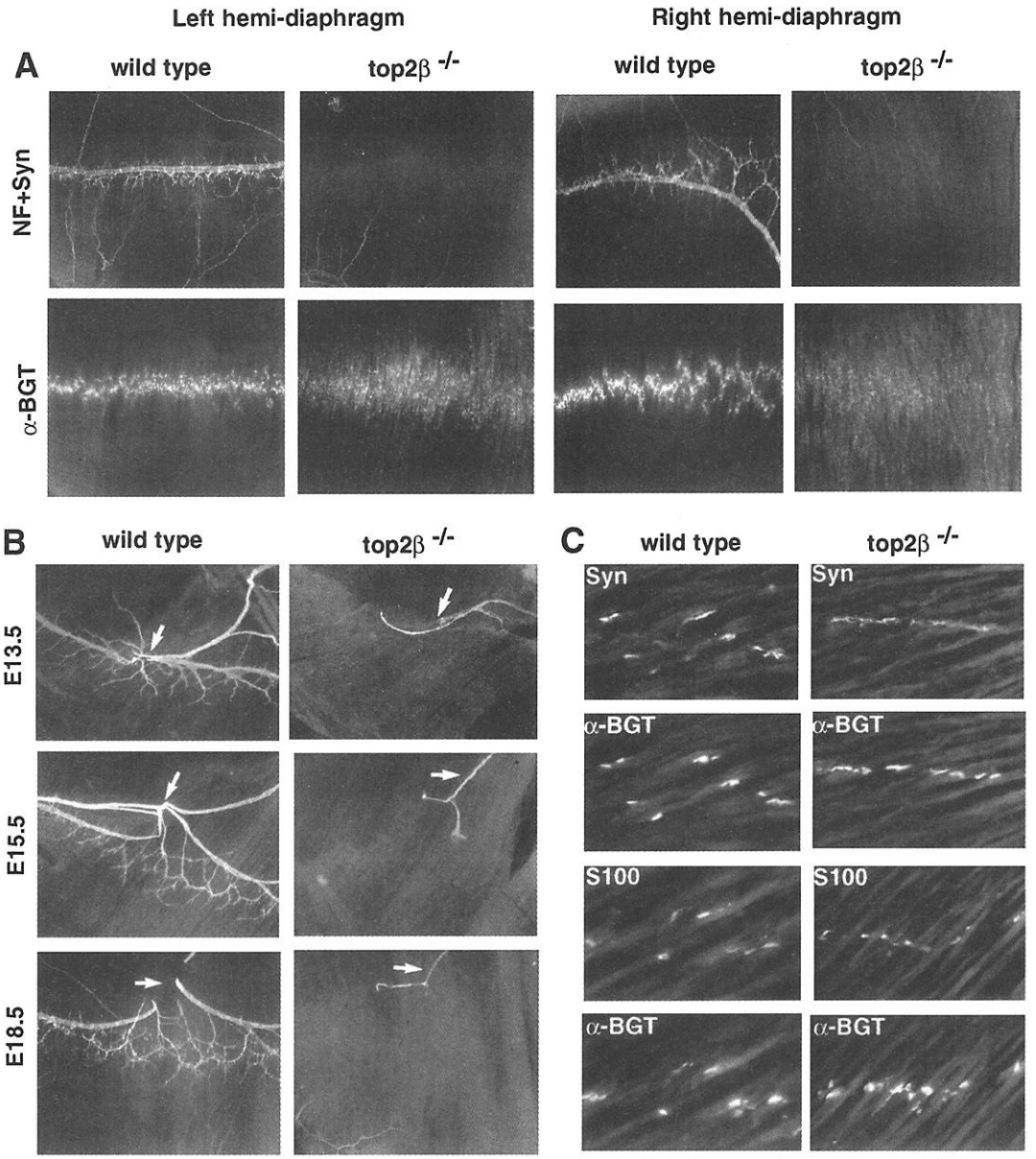

Fig. 2. Failure of motor axons to grow and form synapses in the diaphragm muscle of *top2*β$^{-/-}$ embryos. (**A**) Whole mounts of diaphragm muscles from E18.5 embryos, stained with a mixture of primary antibodies to NF and to Syn (Zymed Laboratory) as well as α-BGT, show that motor axons are absent from *top2*β$^{-/-}$ diaphragm muscles. A band of AChR clusters, which is wider than in normal embryos, is present in the central region of *top2*β$^{-/-}$ muscles. Terminal Schwann cells, labeled by antibodies specific to S100 (Dako), are associated with nerve terminals in normal muscle but are absent from diaphragm muscles of *top2*β$^{-/-}$ embryos (*7*). Experimental details are presented in the supplementary Web material (*6*). (**B**) The phrenic nerve (arrow) reaches the diaphragm muscle but fails to grow within the muscle at E13.5, E15.5, and E18.5. The NF-stained axons, present at the edge of the E18.5 WT and *top2*β$^{-/-}$ diaphragm muscle, are probably sensory or autonomic axons, rather than motor axons, because they are absent from embryos at earlier stages. (**C**) Longitudinal sections of intercostal muscles from E18.5 embryos, stained with antibodies to Syn or S100 and α-BGT, show that intercostal muscles are innervated normally.

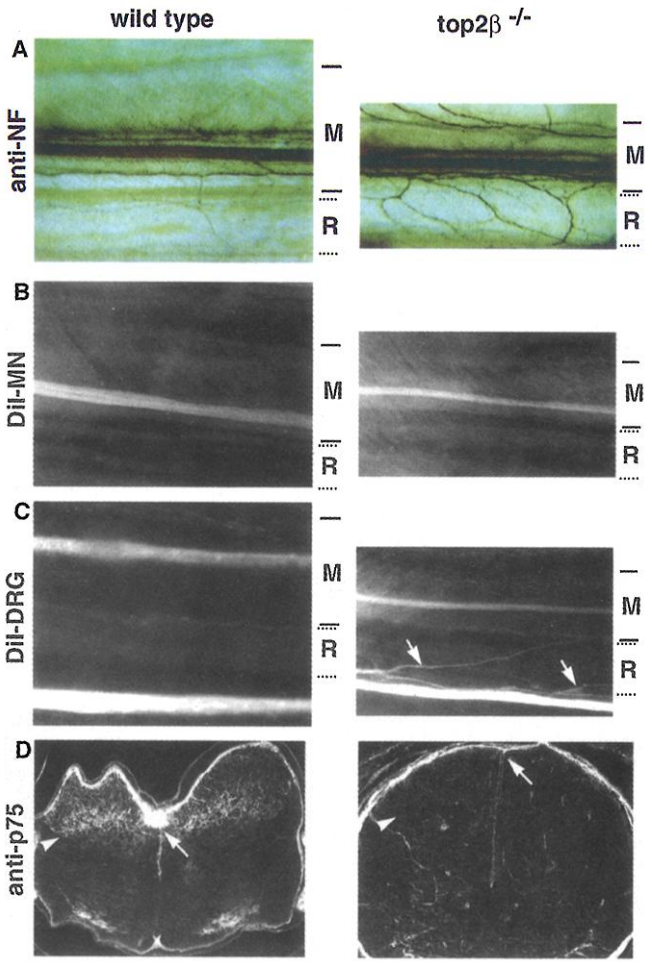

Fig. 3. Defects in sensory projections within intercostal muscles and spinal cord of *top2*β$^{-/-}$ embryos. (**A**) Whole mounts of intercostal muscles from E18.5 embryos, stained with antibodies to NF, show that NF-stained axons grow aberrantly across intercostal muscles and ribs. M and R mark the muscle and rib regions, respectively. (**B**) Motor axons of E18.5 embryos, labeled by injecting DiI into the ventral lateral spinal cord (DiI-MN), project normally in intercostal muscles. (**C**) Sensory axons, labeled by injecting DiI into the dorsal root ganglia (DiI-DRG), project ectopically across the ribs (arrows). Fewer ectopic sensory axons are seen in *top2*β$^{-/-}$ embryos by DiI labeling (C) than by NF staining (A), owing to the low DiI-labeling efficiency of sensory neurons. (**D**) Cross sections of the spinal cord from E18.5 embryos stained with antibodies to p75, which stains sensory as well as motor neurons, show that the dorsal column (arrows) is absent in *top2*β$^{-/-}$ embryos. Nociceptive sensory axons, which grow and terminate within the dorsal horn of the spinal cord in WT embryos (arrowheads), are also absent in *top2*β$^{-/-}$ embryos.

flect a repair deficiency in their absence. It has been suggested that neurons may be more sensitive to repair deficiency than other cell types (*15*). Thus, the observed neural defects in IIβ mutant embryos might be related to the plausible involvement of IIβ in DNA repair (*17*). In budding yeast, DNA topoisomerases I and II suppress mitotic recombination in the ribosomal RNA gene cluster (*18*), and inactivation of IIβ could accentuate genome instability in neurons. The possible involvement of IIβ in gene expression, especially in nonproliferating cells like neurons that express no IIα, also deserves consideration in view of recent findings that eukaryotic type II DNA topoisomerase can form complexes with proteins implicated in gene expression (*19*) and chromatin remodeling (*20*).

References and Notes

1. Reviewed in C. A. Austin and K. L. Marsh, *Bioessays* **20**, 215 (1998); J. C. Wang, *Annu. Rev. Biochem.* **65**, 635 (1996).
2. S. DiNardo, K. Voelkel, R. Sternglanz, *Proc. Natl. Acad. Sci. U.S.A.* **81**, 2616 (1984); C. Holm, T. Goto, J. C. Wang, D. Botstein, *Cell* **41**, 553 (1985); T. Uemura *et al.*, *Cell* **50**, 917 (1987).
3. Reviewed in M. Yanagida and R. Sternglanz, in *DNA Topology and Its Biological Effects*, N. R. Cozzarelli and J. C. Wang, Eds. (Cold Spring Harbor Laboratory Press, Cold Spring Harbor, NY, 1990), pp. 299–320.
4. M. Chen and W. T. Beck, *Oncol. Res.* **7**, 103 (1995); S. Dereuddre, S. Frey, C. Delaporte, A. Jacquemin-Sablon, *Cancer Res.* **57**, 4301 (1997); P. Grue *et al.*, *J. Biol. Chem.* **273**, 33660 (1998).
5. B. Hogan, R. Beddington, F. Constatini, E. Lacy, *Manipulating the Mouse Embryo: A Laboratory Manual* (Cold Spring Harbor Laboratory Press, Cold Spring Harbor, NY, 1994)
6. Supplemental Web material is available at www.sciencemag.org/feature/data/1045398.shl.
7. X. Yang, W. Li, E. D. Prescott, S. J. Burden, J. C. Wang, data not shown.
8. P. Godement, J. Vanselow, S. Thanos, F. Bonhoeffer, *Development* **101**, 697 (1987); M. G. Honig and R. I. Hume, *Trends Neurosci.* **12**, 333 (1989).
9. T. M. DeChiara *et al.*, *Cell* **85**, 501 (1996).
10. J. Lewis, A. Chevallier, M. Kieny, L. Wolpert, *J. Embryol. Exp. Morphol.* **64**, 211 (1981); B. Kablar and M. A. Rudnicki, *Dev. Biol.* **208**, 93 (1999).
11. J. R. Sanes and J. W. Lichtman, *Annu. Rev. Neurosci.* **22**, 389 (1999).
12. P. E. Williams and G. Goldspink, *J. Cell Sci.* **9**, 751 (1971).
13. C. P. Ordahl and N. Le Douarin, *Development* **114**, 339 (1992); C. P. Ordahl and B. A. Williams, *BioEssay* **20**, 357 (1998); reviewed in B. Christ and C. P. Ordahl, *Anat. Embryol.* **191**, 381 (1995).
14. S. Dietrich, F. R. Schubert, C. Healy, P. T. Sharpe, A. Lumsden, *Development* **125**, 2235 (1998).
15. Y. Gao *et al.*, *Cell* **95**, 891 (1998); D. E. Barnes, G. Stamp, I. Rosewell, A. Denzel, T. Lindahl, *Curr. Biol.* **8**, 1395 (1998).
16. K. M. Frank *et al.*, *Nature* **396**, 173 (1998).
17. O. Popanda and H. W. Theilmann, *Carcinogenesis* **13**, 2321 (1992); H. W. Thielmann, O. Propanda, H. Gersbach, F. Gilberg, *Carcinogenesis* **14**, 2341 (1993); K. Yamane, M. Kawabata, T. Tsuruo, *Eur. J. Biochem.* **250**, 794 (1997).
18. M. F. Christman, F. S. Dietrich, G. R. Fink, *Cell* **55**, 413 (1988); R. A. Kim and J. C. Wang, *Cell* **57**, 975 (1989).
19. M. Kobayashi *et al.*, *Mol. Cell. Biol.* **18**, 6737 (1998).
20. P. D. Varga-Weisz *et al.*, *Nature* **388**, 598 (1997).

21. We thank G. Li, A. McMahon, and E Robertson for materials and advice, H. Warren for help in pathological examinations of mice, and A. Sharpe and L. Du for performing blastocyst injections. The gifts of antibodies from T. Jessell and M. Chao are gratefully acknowledged. We also thank M. Matise for advice on DiI labeling. Supported by a NIH postdoctoral fellowship to X.Y. (NS10537) and by NIH research grants to S.J.B. (NS27963 and NS36193) and to J.C.W. (CA47958 and GM24544).

13 September 1999; accepted 29 November 1999

Tbx5 and the Retinotectum Projection

Kazuko Koshiba-Takeuchi,[1]* Jun K. Takeuchi,[1]* Ken Matsumoto,[1] Tsuyoshi Momose,[1] Kenichiro Uno,[1] Veit Hoepker,[2] Keiko Ogura,[1] Naoki Takahashi,[1] Harukazu Nakamura,[3] Kunio Yasuda,[1] Toshihiko Ogura[1]†

Dorsal and ventral aspects of the eye are distinct from the early stages of development. The developing eye cup grows dorsally, and the choroidal fissure is formed on its ventral side. Retinal axons from the dorsal and ventral retina project to the ventral and dorsal tectum, respectively. Misexpression of the *Tbx5* gene induced dorsalization of the ventral side of the eye and altered projections of retinal ganglion cell axons. Thus, Tbx5 is involved in eye morphogenesis and is a topographic determinant of the visual projections between retina and tectum.

Dorsal (medial) and ventral (lateral) aspects of the eye are distinct from early stages of development, and retinal axons project in an organized topographic manner (*1*, *2*). Chick *Tbx5* gene, a member of the T-box transcription factor family, is expressed in the dorsal